Determining total emissions and environmental drivers of methane flux in a Lake Erie estuarine marsh: The Old Woman Creek Wetland

A.Camilo Rey-Sanchez[1,2]

1 - Department of Civil and Environmental Engineering and Geodetic Science, The Ohio State University, Columbus, Ohio, USA.

2- Environmental Science Graduate Program, The Ohio State University, Columbus, OH 43210 USA.

ABSTRACT

Estuarine marshes can act as an important ecosystem for carbon storage and flux. We monitored CH_4 and CO_2 fluxes in Old Woman Creek, an estuarine wetland of Lake Erie, Ohio. The eddy covariance (EC) technique was used to measure fluxes of CH_4 and CO_2 continuously during the growing seasons of 2015 and 2016. Simultaneously, monthly sampling of gas exchange was conducted using accumulation chambers in four distinct land-cover types in the wetland: Open water, emergent vegetation (*Typha spp*.), floating vegetation (*Nelumbo spp*.) and mud flats. Chambers and EC measurements were combined to provide estimates of the continuous contributions of each land cover to the total methane emissions of the wetland. In addition, water and meteorological measurements were used to determine the most important environmental drivers of methane flux in the wetland. We found an average rate of emission from the *Typha* patch of 1.9 g CH_4 m^{-2} d^{-1}, which was much higher than rates reported in similar emergent vegetation types in other wetlands. Mud flats had the highest rates of CH_4 emission, followed by *Nelumbo*, and *Typha* patches, and Open water. Mud flats contributed 6.8% of the total CH_4 emissions of the wetland despite occupying only 1.5% of the wetland area, whereas open water

contributed 16.1% despite occupying 47% of the wetland area. Water temperature, and wind speed were the strongest environmental drivers of CH_4 flux to the atmosphere. Carbon fluxes were strongly correlated to methane fluxes. Fluctuating water levels above the wetland's surface had a weak effect on overall CH_4 emissions in the wetland. Providing an empirical model that predicts the influence of different environmental drivers on the emissions of methane in the wetland, can aid in the design of estuarine wetlands that retain nutrients and reduce coastal eutrophication while minimizing greenhouse gas emissions.

Keywords: Wetland, methane, estuary, carbon, environmental drivers, marsh.

Introduction

Estuaries provide many beneficial ecosystem services. Estuaries process upland river water before they spill into lakes or oceans (Larson et al., 2013). By processing transported nutrients, they help reduce the eutrophication of coastal waters and thereby the occurrence of harmful algae blooms (Horne, 2000; Michalak et al., 2013). Estuarine wetlands also serve an important role in the natural carbon cycle (McLeod et al., 2011). Wetlands can sequester large amounts of carbon due to their low soil oxygen contents that restricts the decomposition of biomass by aerobic microbes. In wetlands, including estuarine ones, carbon in the form of carbon dioxide (CO_2) is also assimilated by plant photosynthesis. In most wetlands, there is a net negative flux of CO_2, which means that more carbon enters the ecosystem through gross primary production (*GPP*) than carbon leaves through ecosystem respiration (R_e) (Bridgham et al., 2006; Mitsch et al., 2013). Estuarine wetlands have the potential to become even more productive than other classes of wetlands due to nutrient rich waters that increases wetland's plant growth (Horne, 2000) and trapping of suspended matter and its associated organic carbon, which increases the long-term

carbon sequestration pool (McLeod et al., 2011). However, the same low oxygen conditions that slow decomposition make wetlands sources of methane (CH_4).

Temperature is perhaps the most commonly cited driver of CH_4 emissions. Microbial processes are directly dependent on temperature, which increases their metabolic rates (Bohn et al., 2007; Kim et al., 1999; Segers, 1998). However, it's linkage to CH_4 emissions is complex due to the competing interaction of anaerobic methanogenesis and aerobic methanotrophy, both of which are stimulated by higher temperatures. Water level is commonly cited as a driver of CH_4, typically due to its association with oxygen availability (Kettunen, 2003; White et al., 2008). Oxygen is the preferred terminal electron acceptor for most methanotrophs, which can oxidize 60-90% of the methane produced in wetlands before it can escape to the atmosphere (Le Mer and Roger, 2001). It has been shown that intermittent flooding can reduce methane emissions relative to permanently flooded wetlands (Altor and Mitsch, 2006), but few studies have examined the effect of short time scale variations of water level on permanently flooded, non-tidal marshes. The availability of labile carbon substrate concentration in the soil also plays a crucial role in the production of methane (Sha et al., 2011; Updegraff et al., 1995), typically modeled as substrate-limited Monod kinetics. The pH can also have an influence on methane emissions as methanogens prefer neutral to slightly alkaline conditions (Wang et al., 1993).

Wetlands are often composed of a mosaic of different land cover types, including open water, emergent vegetation, floating vegetation, mud flats, and dry upland. The rates of CH_4 emission among these land covers can be very variable and their arrangement and relative coverage can strongly influence the total methane emissions from the wetland site as a whole (Matthes et al., 2014; Morin et al., 2017). The presence of plants can increase the methane emission rates by a factor of 3-4 in comparison to areas within the wetland with no vegetation (Hamilton et al.,

1994) and the type and composition of plants within a wetland also have an important effect on methane emissions (Baldocchi et al., 2012; Forbrich et al., 2011; Leppala et al., 2011; Sachs et al., 2010).

There are several methodologies to quantify CH_4 fluxes. The most common one uses non-steady-state chambers, in which the rate of accumulation of a gas in the headspace of a chamber with known volume provides the flux rate. Chambers are relatively simple, low-cost, and can work in a wide range of applications and ecosystems. Chambers are, essentially, point measurements, and thus, provide spatially detailed observations of the flux rates of particular land-cover types, but over a small number of spatially replicated points. When the chamber deployment is done manually and is not automated, they are limited to a very small and intermittent temporal representation. The eddy covariance approach combines high-speed wind and gas concentration data to determine the site level fluxes at a high temporal resolution (typically 10 – 20 Hz processed to half-hourly block averages). The eddy covariance approach measures a mixture of gases originating from a source footprint area that changes with wind speed, direction and turbulence mixing of the atmospheric boundary layer (Detto et al., 2006; Hsieh et al., 2000; Kljun et al., 2004), and often includes various land-cover types that make up the entire site.

In this study we use the approach of Morin et al. (2017) that combines point-wise flux rate estimates from each land-cover type using non-steady-state chamber campaigns, and continuous site-level eddy covariance measurements. By combining these two data streams, it is possible to estimate the separate contributions of different land cover types throughout the site, and provide an integrated whole-site-level estimate of methane flux from the wetland. We studied the Old Woman Creek National Estuarine Research Reserve wetland (OWC), a natural estuarine marsh in Northern Ohio at the coast of Lake Erie (Fig. 1). The first objective of this study is to calculate

the total summer-time emissions of CH_4 from the OWC wetland, by integrating the contributions of different land cover types. The second objective is to identify the most important environmental drivers of CH_4 flux and identify environmental variables that are most strongly correlated with methane flux, and thus develop an empirical model of methane emissions in the wetland

2. Materials and methods.

2.1. Study site

The Old Woman Creek (OWC), in Northern Ohio, is a State Nature Preserve, part of NOAA's National Estuarine Research Reserve (NERR) network. OWC includes 61 Ha of natural wetland area managed by NOAA and the Ohio Department of Natural Resources. There are four main land-cover types in the wetland: 1) Open water, 2) mud flats, 3) Emergent vegetation: a mix of emergent vegetation dominated by *Typha* spp with a small amount of *Phragmites* spp., (for simplicity, we name this land-cover type – *Typha*) and 4) floating-leaf vegetation dominated by *Nelumbo lutea.* Fig. 1 shows the land cover arrangement for the period of the study. Water flows into the wetland from Old Woman Creek as it travels northwards into Lake Erie (Fig. 1). A natural sand barrier acts as a levee that intermittently blocks the exchange of water between Lake Erie and the estuary. Typically, the sand barrier limits the flow from the wetland into Lake Erie (Tomaszek et al., 1997), especially during summertime low-flow periods. Periodically, during storms in the lake, the sand barrier ruptures and allows a rapid flux of water between the wetland and Lake Erie. With the exception of the open-water area in the main channel, most of the wetland is shallow, no deeper than 0.5 m (Whyte et al., 2008).

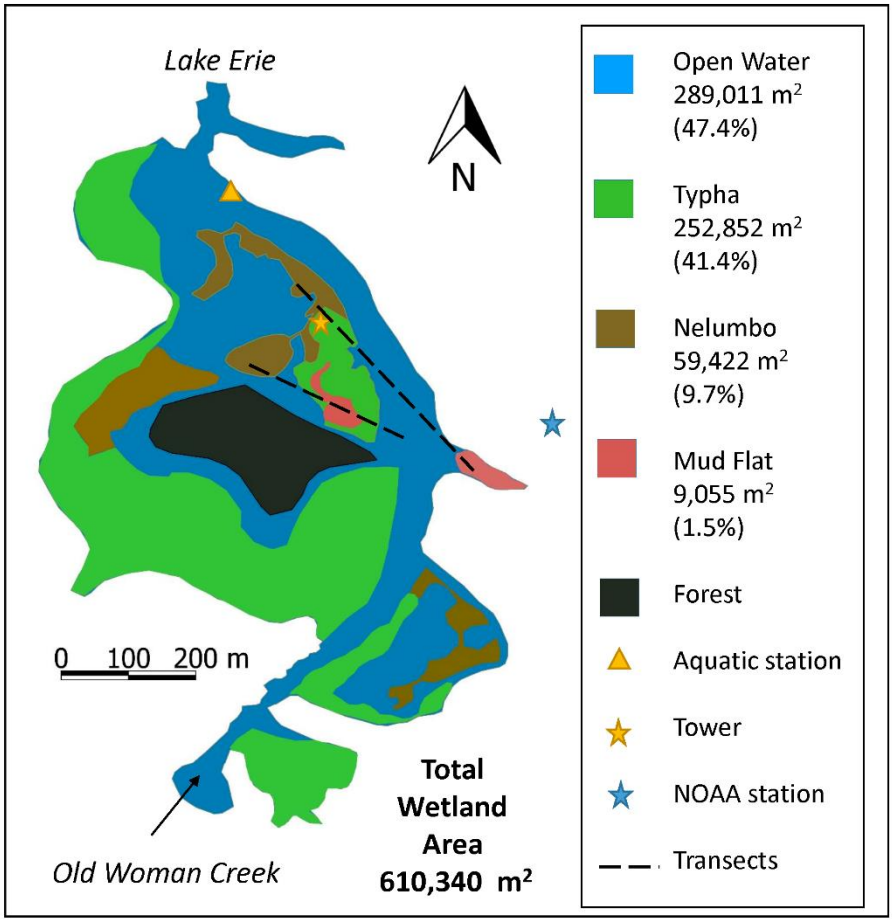

Figure 1. Map of the study site showing the area distribution of each of the four predominant land covers and the meteorological, flux and aquatic stations used in the study. The dotted lines indicate the chamber measurement transects. The area calculation was done by interpretation of Google Earth satellite imagery for the year 2015 and field corroboration.

2.2. Meteorology and flux tower

An eddy-covariance tower was installed in the center of the wetland to measure both meteorological conditions and fluxes of carbon and water from June to October 2015 and from April to October 2016. The meteorological station consisted of one temperature and humidity sensor (HMP45 – Vaisala Inc., Vantaa, Finland) located at approximately 2.5 m above water level and a network of seven temperature sensors (107-L Temperature Sensors – Campbell Scientific, Inc. Logan, UT). Six of these sensors were positioned in three different land cover types (open water, *Typha* and *Nelumbo*), measuring soil temperature at 10 (ST_{10cm}) and 40 cm

(ST_{40cm}) below the soil surface and the final temperature sensor was positioned in the water column, 30 cm above the soil surface. These data were recorded every 1 min and later transformed into 30 min averages. ST_{10cm} and ST_{40cm} for the wetland were calculated as an average of the three temperature sensors located at the different positions.

The flux tower consisted of an infrared gas analyzer (IRGA) for CO_2/H_2O and CH_4 (LI-7500, LI-7700, respectively – LiCOR Bioscience, Lincoln NE), as well as a 3D ultrasonic anemometer (CSAT3 – Campbell Scientific, Inc. Logan, UT). The sensors were positioned 2.7 m above the mean water level of the wetland. All flux variables were recorded with a frequency of 10 Hz. Meteorological and flux data were collected on a datalogger (CR3000, Campbell Scientific, Inc. Logan, UT) connected wirelessly to a computer in the facilities of OWC via FM radio (RF450 – Campbell Scientific, Inc. Logan, UT). After collection at 10 Hz, data were binned into half hourly averages and fluxes.

Additional meteorological data were obtained from a NOAA-operated weather station located 411 m from the wetland (NOAA station, Fig. 1). From this station, we obtained photosynthetic active radiation (*PAR*), relative humidity (*RH*), air temperature (*Tair*), wind speed (*u*), wind direction (*WD*), and cumulative precipitation at a temporal frequency of 15 minutes. An aquatic monitoring station located 303 m from the tower (Fig. 1) provided 15 min averages of water temperature (*WT*), water level, pH, dissolved oxygen (*DO*) and turbidity.

2.3. Chamber measurements

We used non-steady state chambers to measure CO_2 and CH_4 fluxes at the four land cover types in the wetland. The chamber sampling campaign occurred monthly, from June to October 2015 and from May to October 2016. We created two transects along the wetland, each comprising all

four land cover types (Fig. 1). *Nelumbo* was not sampled in June 2015 and the second transect only included mud from June 2016 onwards. As all sites featured some standing water throughout the sampling campaign, the land covers were sampled by boat when possible. Two chambers were used at each point within each transect. Seven samples per chamber were collected every 5 minutes, starting at time 0, for a total of 30 min of sampling. The gas extracted from the chamber was injected into 10 ml evacuated vials, and later taken to the lab to be analyzed on a gas chromatograph (Shimadzu GC-2014, Shimadzu Scientific Instruments, Kyoto, Japan). The procedure for calculation of fluxes, calibration of the instruments and correction for drifts of the gas chromatograph is fully described in Morin et al. (2017), and based on (Nahlik and Mitsch, 2010; Sha et al., 2011). We incorporated selection criteria for rejecting outliers from individual chamber measurements: if the r^2 value for the linear regression between the accumulation rates over 30-minutes was not sufficiently high ($r^2 \geq 0.85$), we removed the point with the highest residual value from the regression. This was done up to twice per chamber. If three points were removed, the entire chamber observation was rejected.

2.4. Flux calculations from eddy covariance

We applied quality control and despiking protocols to the high frequency measurements as described in Morin et al. (2014b). Wind data was subjected to a 3D rotation to force the mean vertical and crosswinds components to zero (Finnigan et al., 2003). A correction was applied to the temperature measurements from the sonic anemometer to account for changes in air density (Kaimal and Gaynor, 1991). Following the procedure of Morin et al. (2014b), a lag correction was applied to account for the separation distance between the sonic anemometers and the IRGAs, and a spectral correction was applied to correct for the temperature dependence of the absorption spectrum of CO_2, CH_4, and water vapor. CO_2 and CH_4 concentrations were applied

WPL corrections to account for the changes in air density (Webb et al., 1980). Data was processed to half hourly means and filtered based on a friction velocity (u^*) threshold. We used an empirical approach for defining a threshold that indicates insufficient level of turbulent mixing below which data is rejected (Reichstein et al., 2005). The minimum value of u^* used in this study was 0.2 m s^{-1}.

In the case that our observations included gaps, typically due to power supply problems, missing meteorological data were replaced with data from the NOAA station, with empirical corrections applied based on the linear relationship between the variables when both were available. When not available, data was gap-filled using a simple bi-linear, periodic trended interpolation relationship (Morin et al., 2014b) that took into account both the diurnal variation and the closest available values of the variables to be gap-filled.

2.5. Modelling and gap-filling of fluxes

EC measurements of CO_2 flux (*NEE*) was partitioned into Gross Primary Productivity (*GPP*) and ecosystem respiration (R_e). At nighttime, *NEE* was completely attributed to R_e as no photosynthesis is expected in the wetland. An automated neural network (ANN) model (Moffat et al., 2007; Morin et al., 2014a) was trained to determine an empirical model of R_e, as a function of environmental variables, using a subset of available nighttime values. We then used this trained ANN and environmental observations to model R_e at all periods (including daytime). Subsequently, we subtracted the modeled R_e from the observed *NEE* to calculate *GPP* when carbon flux observations where available. A new ANN process was then trained to model daytime *GPP* and used to gap-fill missing *GPP* observations. We used ANN to gap-fill sensible (*H*) and latent (*LE*) heat fluxes as well. The environmental variables that we selected to contribute to the R_e model were: ST_{10cm}, *H*, *LE*, *VPD*, wind speed (*U*), U^* and T_{diff}. Whereas for

193 *GPP* the selected environmental variables included: *VPD*, *H*, T_{diff}, *PAR*, *LE*, Air temperature
194 (T_{air}), *U*, *U** and *RH*. Variables were selected according to their pairwise linear regression with
195 R_e or *GPP*. Following Morin et al. (2014a), we used a step-wise Akaike Information Criterion
196 (AIC)-driven variable selection process to determine which of these variables have a significant
197 and justified contribution to the model as shown in Table 1. Variables that did not reduce the
198 AIC of the model were not included in the final model. For all ANNs, we ran 1000 iterations
199 from which we selected the best 10% based on the r^2 of the model. The ensemble average of
200 these top 100 iterations was used to create the final model and the subsequent gap-filling. We
201 created these ANN-based empirical models of fluxes with the objective of: (1) understanding the
202 relationship between environmental drivers and the fluxes; and (2) creating proxy time series to
203 model fluxes.

204 *2.6. Scaling methodology*

205 To determine the site-level methane budget, we used an expanded version of the fixed-frame
206 eddy-covariance (EC) scaling methodology developed by Morin et al. (2017). Briefly, this
207 method combines EC measurements, with a footprint model, a land cover map, and land-cover
208 specific flux measurements collected using the chamber method, to decompose the EC flux
209 signal into its contributing parts by each land cover type. We used the (Detto et al., 2006)
210 footprint model, which is a 2D expanded version of the Hsieh et al. (2000) formulation. We used
211 monthly varying displacement heights and roughness lengths to account for the growth of *Typha*
212 around the tower. Given the four land-cover types throughout the wetland, at any half hour the
213 flux measured by the tower can be decomposed to the contributions of each land-cover type:

214 $$F_{tower} = F_{op}{}'e_{op} + F_{ty}{}'e_{ty} + F_{ne}{}'e_{ne} + F_{mu}{}'e_{mu} \quad (1)$$

Where *F'* of each land cover type indicates the EC-derived flux rate of that land cover type (where subscripts: *op* = open water, *ty* = *Typha*, *ne* = *Nelumbo*, *mu* = mud flat) and *e* is the fraction that each patch type contributed to the total EC measurement footprint.

Chamber flux data determined the relative flux strengths of fluxes from each land cover type compared to open water fluxes (eq. 2, 3 and 4).

$$m_1 = \frac{F_{ty}}{F_{op}} = \frac{F_{ty}'}{F_{op}'} \tag{2}$$

$$m_2 = \frac{F_{ne}}{F_{op}} = \frac{F_{ne}'}{F_{op}'} \tag{3}$$

$$m_3 = \frac{F_{mu}}{F_{op}} = \frac{F_{mu}'}{F_{op}'} \tag{4}$$

Where F_x is the flux measured by the chamber at each land cover type *x*. Because chamber measurements were taken monthly, the values of *m* varied monthly. Then, by substituting eqns. 2-4 into eq. 1, the chamber-derived flux intensity ratios can be used to translate the total footprint flux to an equivalent open-water flux rate

$$F_{tower} = F'_{op}\, e_{op} + m_1 F'_{op}\, e_{ty} + m_2 F'_{op}\, e_{ne} + m_3 F'_{op}\, e_{mu} \tag{5}$$

Eq. 5 can be solved for F_{op} at any observed half-hour. Similarly, using eq. 1-4, a solvable system of equations can be derived for the relative flux strength of each patch type contributing to the eddy-covariance observation. Multiplying these rates by the actual area of each land-cover type within the whole wetland will yield the fixed-frame total contribution of that land-cover type to the site-level flux.

3. Results

3.1. Daily and diurnal variation of CO_2 and CH_4 fluxes

Our ANN simulated *H* and *LE* very efficiently. The r^2 of the relationship between the values predicted by the ANN and the observed values of *H* and *LE* were 0.84 and 0.86 for 2015, and 0.70 and 0.82 for 2016, respectively. EC-CO_2 flux measurements indicated that *NEE* was greater (more negative, therefore higher photosynthesis) in 2016 than in 2015 whereas CH_4 emissions were higher in 2015 than in 2016 (Fig. 2). The daily mean NEE was -0.47 $\pm$0.80 μmol m^{-2} s^{-1} (mean $\pm$ std), comprised of daily mean *GPP* of -2.81 $\pm$1.27 μmol m^{-2} s^{-1} and daily mean R_e of 2.35 $\pm$1.51 μmol m^{-2} s^{-1}. Values of R_e were high when compared to other ecosystem types, likely due to the soil conditions, which is rich with dissolved organic carbon, bringing the seasonal total *NEE* close to zero. The correlation between observed and ANN-predicted values of *NEE*, *GPP* and R_e achieved high coefficients of determination (r^2= 0.84, 0.79, 0.68 for 2015 and 0.83, 0.69 and 0.52 for 2016, respectively). Daily averages of *DO* for the period from June to October were not significantly different between 2015 and 2016 (t-test, p=0.65), however, for the same period water temperature was significantly higher in 2016 than in 2015 (t-test, p<0.01). Water temperature had an inverse relationship with *DO*, with the lowest *DO* occurring in the warmest months. Water level was highly variable and tended to increase from spring to fall in both years.

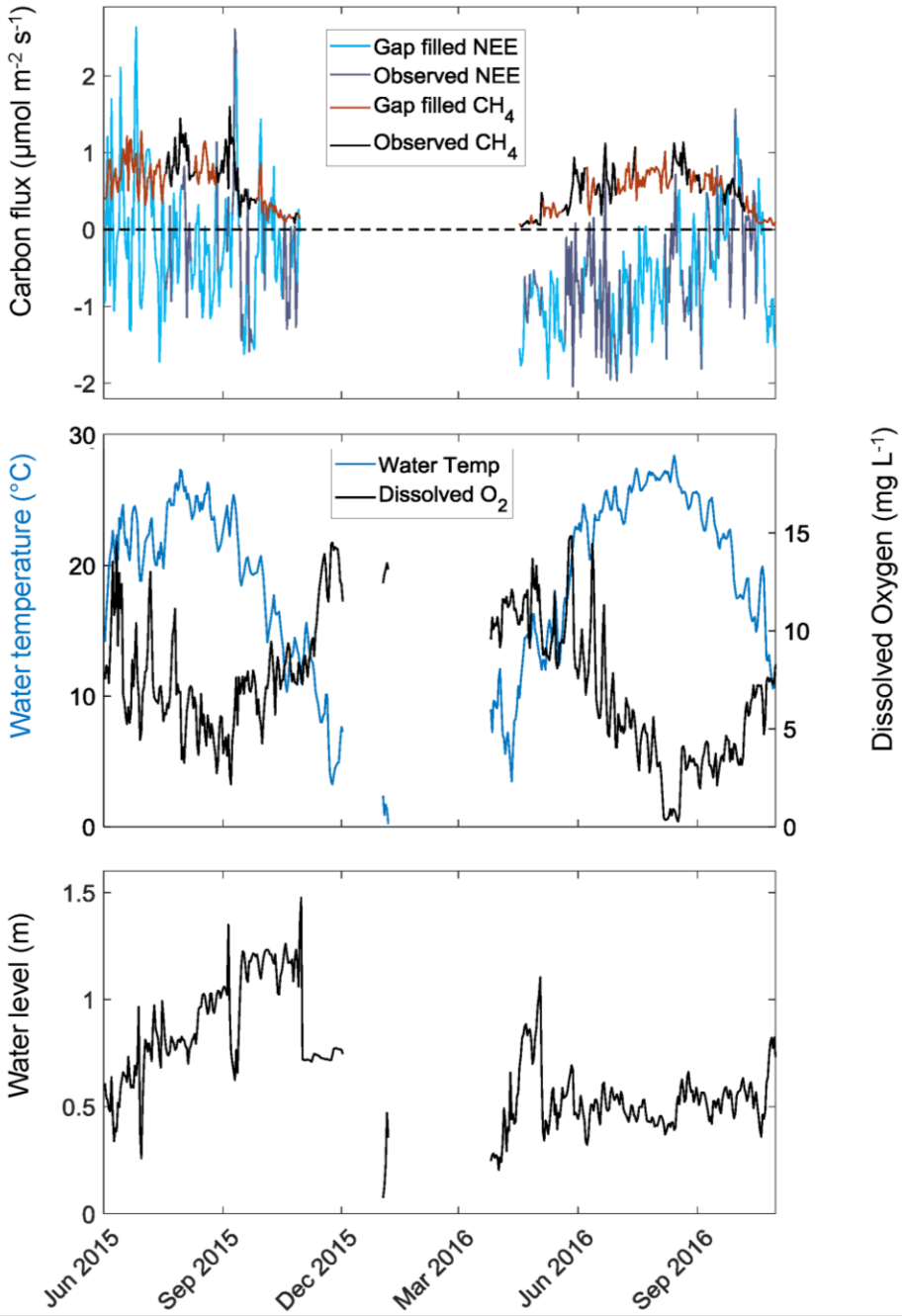

250

251 *Figure 2. Temporal variation of diurnal averages of a) Net Ecosystem Exchange and methane. The gap-*
252 *filled values represent averages for which more than 50% of the data for that day was gap-filled. b)*
253 *Water temperature and dissolved oxygen and c) water level above the soil surface around the tower.*

254

255 The daily mean of CH_4 flux was 0.55 $\pm$ 0.31 µmol m^{-2} s^{-1} (Fig. 2), spanning a range from 0.03 to

256 1.60 µmol m^{-2} s^{-1}. Fig. 3 shows the observed diurnal cycles of *CH_4* flux and *NEE* from both 2015

and 2016. The diurnal cycle of CH_4 flux was characterized by a sharp increase in flux around the mid-morning, approximately from 7:00 to 10:00 AM. In addition, CH_4 fluxes tended to be lower right after the mid-morning spike and during the first half of the night, whereas in the second half of the night CH_4 emissions tended to be slightly higher. The diurnal cycle of *NEE* had a more sinusoidal shape, as is typical, due to the competing processes of photosynthesis and respiration. During the night, *NEE* reached an average of 4 to 5 μmol m^{-2} s^{-1}, whereas during the day maximal *NEE* was close to -5 μmol m^{-2} s^{-1}.

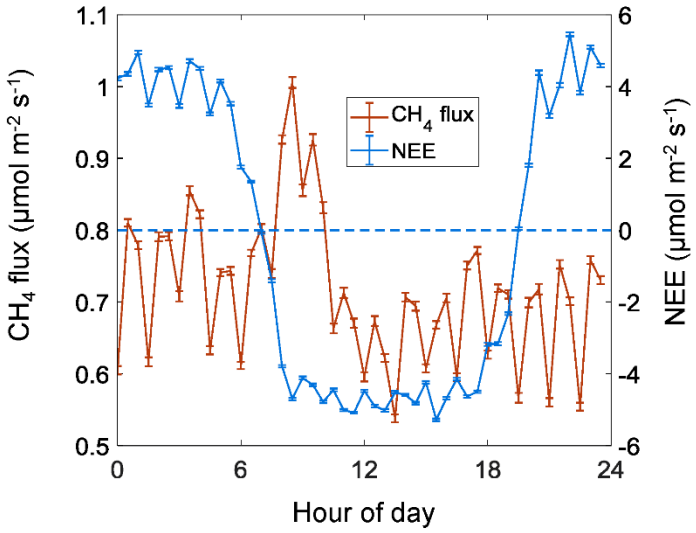

Figure 3. Diurnal cycle of methane and CO_2 flux for half hour intervals as measured by the eddy covariance tower. The values are non-gap-filled averages for 2015 and 2016. Error bars are the standard error.

3.2. Environmental predictors of CH_4 flux

During daytime, water temperature (*WT*) had the highest correlation with CH_4 flux. The second most important variable was *GPP*, followed by *u*, *LE* and *H* (Table 1). Each of the subsequent variables in the model (Table 1) increased the r^2 slightly, until FP_{open}. The remaining variables,

including *WL* had significant, though very small, contribution to the model. Overall, r^2 of the daytime CH_4-flux model improved from 0.56 in the stepwise linear model to 0.86 using ANN.

During nighttime, the most important variable in the stepwise linear model of CH_4 flux was R_e (Table 1). As with the daytime fluxes, *WT*, *u* and *LE* were also important in determining the CH_4 flux. In contrast, *DO* and *WL* had a stronger effect on CH_4 fluxes during nighttime than during daytime. Other variables, such as F_{open}, atmospheric pressure (P_{atm}), *u**, half-hourly change in atmospheric pressure (ΔP_{atm}) and FP_{Typha} were rejected in the ANN as their addition to the ANN process did not significantly improve the model.

*Table 1. Results of the statistical tests to determine the most important drivers of the methane flux models: Correlation coefficients (r) of the pairwise linear relationship indicate the strength and sign (positive or negative) of the relationship. Stepwise linear multivariate and stepwise hierarchical Neural Network models test the effects of each variable through their incremental improvement of the cumulative coefficient of determination (r^2) and Akaike Information Criterion (AIC) values. A * next to an AIC value indicates that the variable was rejected (due to a rise in AIC from the previous variable). The ANN models included only the variables that had a significant effect on the stepwise linear model.*

		Pairwise linear	Stepwise Linear		Neural Network	
		r	Cum. r^2	Cum. AIC	Cum. r^2	Cum. AIC
Day	*WT*	0.49	0.28	22503	0.42	38557
	GPP	-0.33	0.27	19315	0.46	37483
	U	-0.32	0.32	18622	0.53	35048
	LE	0.41	0.39	17636	0.56	33846
	H	-0.33	0.43	16952	0.63	30899
	VPD	0.29	0.45	16547	0.71	27046
	T_{air}	0.49	0.48	15978	0.75	24234
	*u**	-0.03	0.50	15702	0.78	22180
	DO	0.12	0.51	15559	0.80	20825
	ST_{10cm}	-0.14	0.53	15065	0.81	19445
	FP_{open}	0.04	0.55	14959	0.82	19116
	ΔP_{atm}	-0.04	0.55	14848	0.82	18613
	P_{atm}	-0.26	0.56	14829	0.83	18373
	FP_{Typha}	0.04	0.56	14828	0.86	15160
	WL	-0.14	0.56	14772	0.86	14114
	PAR	-0.10	0.56	14776*	-	-
Night	R_e	0.54	0.31	17047	0.42	38405
	W	0.59	0.42	15191	0.61	31832

U	-0.31	0.45	14875	0.67	28889
LE	0.35	0.47	14570	0.66	29352*
DO	0.14	0.49	14333	0.79	21770
VPD	0.21	0.50	14107	0.81	19796
T_{air}	0.49	0.53	13666	0.82	19017
H	-0.39	0.55	13324	0.80	20291*
WL	-0.25	0.56	13163	0.83	17528
FP_{open}	-0.02	0.60	12840	0.80	20573*
P_{atm}	-0.22	0.61	12756	0.83	18175*
*u**	-0.20	0.61	12685	0.82	18871*
ST_{10cm}	-0.09	0.61	12645	0.84	17344
ΔP_{atm}	-0.04	0.61	12641	0.83	18189*
FP_{Typha}	0.02	0.61	12636	0.80	20300*
LE	-	-	-	0.84	16725
H	-	-	-	0.84	16497
FP_{open}	-	-	-	0.83	18046*
P_{atm}	-	-	-	0.84	17210*
*u**	-	-	-	0.84	16997*
ΔP_{atm}	-	-	-	0.84	17171*
FP_{Typha}	-	-	-	0.84	16920*

3.3. Spatial variation of CH_4 flux and its effect on the methane budget of the wetland

After the decomposition of the site-level eddy covariance measurements into its land-cover type components, it was clear that there was a large variation in *CH_4* flux among the four land-cover types. The mud flats had the highest rate of methane emissions, reaching daily averages of up to 21 μmol m^{-2} s^{-1}, while the open water areas had the lowest rates, peaking at 0.5 μmol m^{-2} s^{-1}. *Nelumbo* had higher rates of CH_4 emission than *Typha* in 2015 but in 2016, *Typha* had higher rates, except for a short period early in the growing season (April and May). The mud flats had one period of high CH_4 emissions in early 2015 and 2 periods of high emissions in 2016 in May and August.

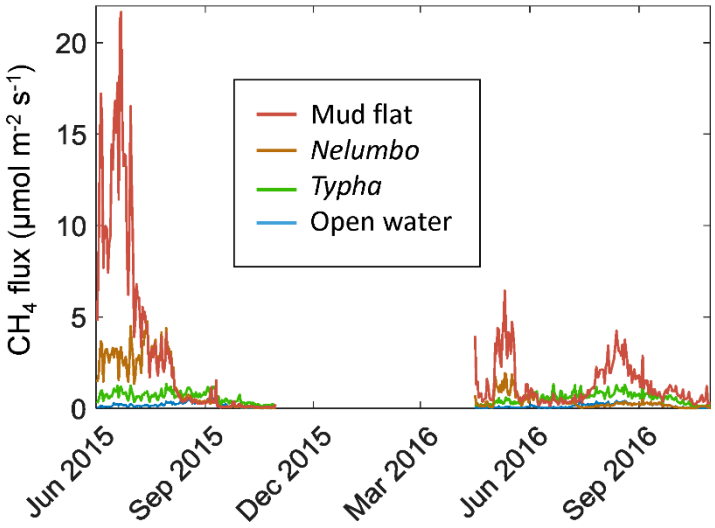

Figure 4. Daily averages of methane flux per land cover for the time of study. The values were calculated based on the chamber measurements and temporally corrected using the tower data, using the methodology develop by Morin et. al (2017).

The effect of variation in CH_4 flux rates among different land cover types on the overall methane budget of the wetland is shown in Fig 5. Due to its low CH_4 emission rates, the contributions of open water to the total CH_4 emissions were relatively low (16.1 %), despite having the largest land coverage type in the site (47 % of the wetland area). In contrast, mud flats contributed significantly to the total CH_4 emissions of the wetland (6.8%), especially in June 2015 (22.2%), despite occupying only 1.5 % of the wetland area. The contributions of *Nelumbo* in 2015 were also large (15%), although it occupies a relatively small area (9.7 % of the wetland). Overall, due to its large areal coverage, *Typha* vegetation was the land-cover type from which most of the

312 CH_4 emissions originated, ranging from 34% in June 2015 to 80% in October 2015.

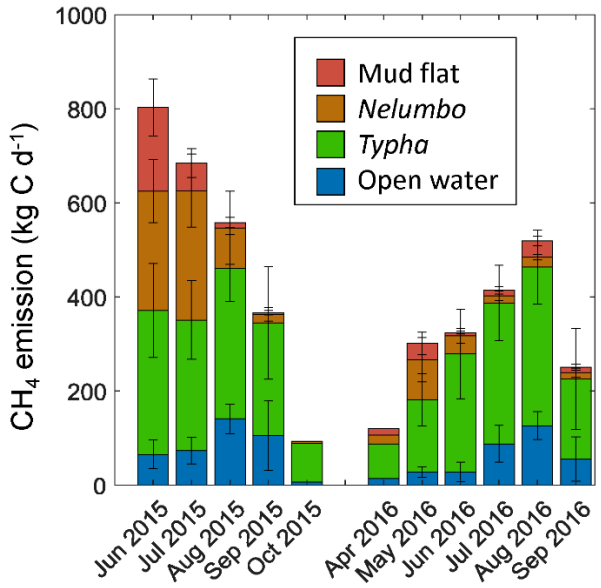

313

314 *Figure 5. Contributions of each land cover to the total methane emissions of the wetland. In this graph,*
315 *the fluxes from the previous graph were normalized by the area of each land cover. Note that although*
316 *the mud flats occupy only 1.5 % of the wetland area, it contributed 22.2% of the total methane emissions*
317 *in June 2015. The error bars are the standard deviation of the daily averages.*

318

319 **4. Discussion**

320 *4.1. The environmental drivers of methane flux*

321 We found that temperature is one of the main drivers of methane emissions, consistent with the
322 findings in other wetlands (Bloom et al., 2010; Bohn et al., 2007; Hatala et al., 2012b). Unlike
323 other studies, however, it was the water temperature and not the soil or air temperature that had
324 the highest correlation with methane emission rates in the OWC wetland. *WT* ranked first for the
325 daytime flux model and second for nighttime flux model (Table 1), whereas ST_{10cm} ranked 10th in
326 the daytime and 13th in the nighttime. The slopes of the pairwise relationship of *WT* and methane
327 flux were positive, which indicates that higher water temperatures are causing more methane
328 emissions. This result is consistent with the finding of Kim et al. (1999), whom found that the

329 diurnal cycle of water temperature and not that of the sediment temperature was correlated with
330 the diurnal cycle of methane flux. On the other hand, the slope of the relationship between the
331 temperature of the soil and methane flux was negative. This could possibly mean that higher
332 temperatures in the soil are favoring microbial methanotrophy processes at higher rate than
333 methanogenesis.

334 Wind speed was an important variable in the determination of methane fluxes, occupying the
335 third position in the rank for both daytime and nighttime models. In contrast, turbulence mixing,
336 u^*, ranked lower (8^{th} in daytime and 12^{th} in nighttime), opposite to previous reports (Herbst et
337 al., 2011; Morin et al., 2014a). Both variables control the rate of mixing at the top water layer
338 and the degree of gas exchange between the surface and the atmosphere. The higher effect of u
339 rather than u^*, may be a result of the overall uniform effect of wind speed, with the different
340 drag coefficients of each land-cover type making the effect of u^* highly variable among patches
341 and thus, a less consistent predictor of methane fluxes from the overall site.

342 Atmospheric pressure can also play an important role in determining methane fluxes, as it can
343 cause increases in the rates of ebullition (Tokida et al., 2007). We found that lower atmospheric
344 surface-level pressure caused a slight increase in CH_4 fluxes as noted by negative pairwise
345 correlation coefficients for both daytime and nighttime. The slope of the pairwise relationship
346 between ΔP_{atm} and methane flux suggests that a rapid decrease in atmospheric pressure caused an
347 increase in methane emissions.

348 *4.2 Other predictors of methane flux*

349 The second most important predictor of methane flux was CO_2 flux. Specifically, *GPP* during
350 the day and R_e during the night. Though a hypothetical relationship between GPP and methane

flux exist, as GPP provides the dissolved carbon that is rapidly consumed in the pathway that leads to methanogenesis, we do not think that carbon fluxes are direct drivers of methane flux. The negative correlation between *GPP* and methane fluxes indicates that higher rates of photosynthesis (with a negative sign) co-occur in times and places of higher methane emissions. This behavior has been identified in other studies (Bellisario et al., 1999; Hatala et al., 2012a; Kim et al., 1999) and can be attributed to increased methane transport through stomata or aerenchyma, or the addition of root exudates to the soil. During nighttime, the complex network of environmental conditions that influence the microbial processes that control methane production are similarly affecting respiration.

Water vapor flux, *LE*, was also an important predictor of methane flux, ranking fourth for both daytime and nighttime models. The covariance between *LE* on methane fluxes has been attributed to the increased vaporization of molecules at the surface of the water that allows higher volatilization of methane in the turbulently mixed regime (Godwin et al., 2013). However, it is also possible that the cause of the strong relationship between *LE* and CH_4 flux is also related to plant transpiration, as stomatal conductance can be an important driver of CH_4 fluxes (Ding and Cai, 2007; Morrissey et al., 1993).

4.3. Variation in flux rates among land-cover types

There was high spatial variability in methane emissions. The diurnal averages in the mud flats were sometimes one order of magnitude higher than in the other land covers (Fig. 4). Such variation in CH_4 emission due to heterogeneity in land covers has been found in other studies (Nahlik and Mitsch, 2010; Sha et al., 2011). Sha et al. (2011) attributed this variation to differences in the soil chemistry at the study sites. It is possible that part of the variation in methane fluxes that our models did not explain is also related to the chemistry of the soil,

especially, the availability of labile carbon. It is also possible that differences in local conditions and transport processes account for some of these flux-rate differences. For example, we suggest that the depth of the mixed water column above the soil surface can explain the differences in methane emissions between open water and *Typha*. Open water has a deeper water column, which means potentially higher methanotrophy, whereas the water level above the *Typha* is much lower, which could cause less oxygenation during transport through the water column.

The footprint variable, which quantifies the contribution of open water or *Typha* to the total flux signal observed by the tower, provides a proxy for estimating the variation in flux rates among land-cover types. If a certain land-cover type has a much higher flux rate than other land-cover types in the site, its contribution to the footprint will be positively correlated with the total observed EC flux. The percentage of the footprint coming from open water occupied in the model the 11^{th} position during the day and 10^{th} during the night. These ranks are not at the top possibly because the ANN is capturing some components of the variation in the contribution of different land-cover types through other variables, mainly *GPP* and R_e, which ranked much higher. As with methane emissions, land-cover types should similarly affect CO_2 emissions.

4.4. Diurnal and seasonal variation of methane flux

We found a clear peak of methane emissions occurring in the early morning around 8:30 am (Fig. 3). This peak is possibly related to the opening of stomata in the morning after a nighttime accumulation of methane in the plant conductive tissues. Kim et al. (1999) found similar results in a temperate marsh dominated by *Phragmites* vegetation. However, the shape of the cycle and the rates of CH_4 emission in our study were different. Except for the peak in the early morning, we did not find large differences of methane flux between daytime and nighttime, unlike Kim et al. (1999), who found a gradual increase in methane flux after sunrise that decreased in the late

afternoon. We also found marked seasonal variation of methane fluxes, which were lower at the beginning of the growing season, reached a peak in the months of July and August and later decreased in September and October (Fig. 2a). A similar pattern of seasonal methane emissions was also found by Kim et al. (1999).

4.5. High rates of methane emission

We found very high rates of methane emission in the OWC wetland. Despite being a net sink of CO_2 during the growing season (negative total NEE) the amount of carbon leaving the ecosystem in the form of methane was so high that the wetland was a net carbon source to the atmosphere during the growing season (Fig 2). The rate of CH_4 emission in *Typha*, the most common plant in the wetland, was on average 0.58 μmol m^{-2} s^{-1}, reaching maximum diurnal averages of up to 1.4 μmol m^{-2} s^{-1}. In contrast, others reported lower methane emission of 0.47 μmol m^{-2} s^{-1} in a wetland dominated by *Phragmites* (Kim et al., 1999) and 0.43 μmol m^{-2} s^{-1} in the Florida everglades (Burke et al., 1988). Devol et al. (1988) found that the range of methane emission for different aquatic macrophytes in the Amazon was 0.02-0.47 μmol m^{-2} s^{-1}. Seasonally integrated methane emissions were equal to 158.1 g CH_4 m^{-2} for the 5-month period of measurements in 2015 and 121.8 g CH_4 m^{-2} for a 6-month period of measurement in 2016. The latter estimate is much higher than the estimate of 64 g CH_4 m^{-2} found by Kim et al. (1999) for a similar 6-month period of time (April to October) in a *Phragmites*-dominated temperate marsh. We hypothesize that this high rate of methane fluxes in OWC is driven by high input rates to the wetland of dissolved organic carbon and other nutrient from the upstream agriculture-dominated watershed.

4.6. The importance of estuarine marshes

Despite the high rates of methane emission, the OWC wetland is an important sink of phosphates and nitrates (McCarthy et al., 2007). This is particularly important in the Southern coast of Lake Erie in Ohio where there has been a high occurrence of harmful algae blooms due to excess of phosphorus and nitrogen from agricultural runoff (Michalak et al., 2013). We have shown that different land covers have different rates of emission and factoring their contributions correctly is critical to calculating the true carbon budget of a wetland. This information can be useful for the design of estuarine wetlands that maximize nutrient retention, reducing coastal eutrophication, while minimizing minimize greenhouse gas emissions. Although our empirical model, based on physical and biological variables, provided good predictions of CH_4 flux, further understanding of the chemistry and the microbiology of the sediments is needed in order to improve mechanistic process-based models. Such models could predict methane emissions from estuarine wetlands accurately.

5. Conclusions

The rates of methane emission in the OWC are higher than the rates reported in similar wetlands. Water temperature and wind speed were the main environmental drivers of methane flux whereas other variables, such as water level or pH, did not have a strong effect on methane fluxes. Photosynthesis and respiration were highly related to methane flux, which indicated that similar sediment processes and environmental drivers are affecting these fluxes. Land-cover heterogeneity had a strong effect on the methane budget of the wetland. Mud flats had the highest rates of methane emission, while the total contributions of the open water patches were lower, despite occupying almost half of the wetland's area. Accounting for differences in methane flux rates among land-cover types within a wetland and their temporal variation is important to provide accurate estimates of total methane flux.

Acknowledgements

Data from the NOAA weather and water monitoring stations in OWC is available at http://cdmo.baruch.sc.edu/get/export.cfm. Meteorological and flux data from OWC is available through Ameriflux (https://ameriflux.lbl.gov/data/download-data/). We are grateful to Kristin Arend, Frank Lopez, Dr. Dave, and the rest of the OWC management team for site access and logistical support. We thank Austin Rechner, Dominique Haddad, Matthew Right, Sharon Acosta, Golnaz Mirfenderesgi and Chante Vines for their assistance in field measurements. This research was partially supported by Ohio Water Development Authority awards (#6835 and 6560). Data analysis was conducted at the Ohio Supercomputer Center. Graduate student support was provided by the National Sciences foundation via a Doctoral Dissertation Improvement Grant (to THM), by the Department of Energy Office of Science Graduate Research Program, Solicitation 2 (to THM), and by the Fay Fellowship through the OSU Environmental Science Graduate Program (to THM and ACRS). Flux observations and analyses were conducted with partial support from U.S. Department of Energy's Office of Science, Ameriflux Management project.

References

Altor, A.E. and Mitsch, W.J., 2006. Methane flux from created riparian marshes: Relationship to intermittent versus continuous inundation and emergent macrophytes. Ecological Engineering, 28(3): 224-234.

Baldocchi, D. et al., 2012. The challenges of measuring methane fluxes and concentrations over a peatland pasture. Agric. Forest Meteorol., 153: 177-187.

Bellisario, L.M., Bubier, J.L., Moore, T.R. and Chanton, J.P., 1999. Controls on CH4 emissions from a northern peatland. Global Biogeochemical Cycles, 13(1): 81-91.

Bloom, A.A., Palmer, P.I., Fraser, A., Reay, D.S. and Frankenberg, C., 2010. Large-Scale Controls of Methanogenesis Inferred from Methane and Gravity Spaceborne Data. Science, 327(5963): 322-325.

Bohn, T.J. et al., 2007. Methane emissions from western Siberian wetlands: heterogeneity and sensitivity to climate change. Environmental Research Letters, 2(4).

Bridgham, S.D., Megonigal, J.P., Keller, J.K., Bliss, N.B. and Trettin, C., 2006. The carbon balance of North American wetlands. Wetlands, 26(4): 889-916.

Burke, J., Barber, T. and Sackett, W., 1988. Methane flux and stable hydrogen and carbon isotope composition of sedimentary methane from the Florida Everglades. Global Biogeochemical Cycles, 2(4): 329-340.

Detto, M., Montaldo, N., Albertson, J.D., Mancini, M. and Katul, G., 2006. Soil moisture and vegetation controls on evapotranspiration in a heterogeneous Mediterranean ecosystem on Sardinia, Italy. Water Resources Research, 42(8).

Devol, A.H., Richey, J.E., Clark, W.A., King, S.L. and Martinelli, L.A., 1988. Methane emissions to the troposphere from the amazon floodplain. Journal of Geophysical Research-Atmospheres, 93(D2): 1583-1592.

Ding, W.X. and Cai, Z.C., 2007. Methane emission from natural wetlands in China: Summary of years 1995-2004 studies. Pedosphere, 17(4): 475-486.

Finnigan, J.J., Clement, R., Malhi, Y., Leuning, R. and Cleugh, H.A., 2003. A re-evaluation of long-term flux measurement techniques - Part I: Averaging and coordinate rotation. Bound. Layer. Meteorol., 107(1): 1-48.

485 Forbrich, I. et al., 2011. Cross-evaluation of measurements of peatland methane emissions on
486 microform and ecosystem scales using high-resolution landcover classification and
487 source weight modelling. Agric. Forest Meteorol., 151(7): 864-874.
488 Godwin, C.M., McNamara, P.J. and Markfort, C.D., 2013. Evening methane emission pulses
489 from a boreal wetland correspond to convective mixing in hollows. J. Geophys. Res.
490 Biogeosci., 118(3): 994-1005.
491 Hamilton, J.D., Kelly, C.A., Rudd, J.W.M., Hesslein, R.H. and Roulet, N.T., 1994. Flux to the
492 atmosphere of CH4 and CO2 from wetland ponds on the hudson-bay lowlands (HBLS).
493 Journal of Geophysical Research-Atmospheres, 99(D1): 1495-1510.
494 Hatala, J.A., Detto, M. and Baldocchi, D.D., 2012a. Gross ecosystem photosynthesis causes a
495 diurnal pattern in methane emission from rice. Geophys. Res. Lett., 39.
496 Hatala, J.A. et al., 2012b. Greenhouse gas (CO2, CH4, H2O) fluxes from drained and flooded
497 agricultural peatlands in the Sacramento-San Joaquin Delta. Agriculture Ecosystems &
498 Environment, 150: 1-18.
499 Herbst, M., Friborg, T., Ringgaard, R. and Soegaard, H., 2011. Interpreting the variations in
500 atmospheric methane fluxes observed above a restored wetland. Agric. Forest Meteorol.,
501 151(7): 841-853.
502 Horne, A.J., 2000. Phytoremediation by constructed wetlands. Phytoremediation of
503 Contaminated Soil and Water, 13-39 pp.
504 Hsieh, C.I., Katul, G. and Chi, T., 2000. An approximate analytical model for footprint
505 estimation of scaler fluxes in thermally stratified atmospheric flows. Adv. Water Resour.,
506 23(7): 765-772.

507 Kaimal, J.C. and Gaynor, J.E., 1991. Another look at sonic anemometry. Boundary Layer
508 Meteorol., 56: 401-410.
509 Kettunen, A., 2003. Connecting methane fluxes to vegetation cover and water table fluctuations
510 at microsite level: A modeling study. Global Biogeochemical Cycles, 17(2).
511 Kim, J., Verma, S.B. and Billesbach, D.P., 1999. Seasonal variation in methane emission from a
512 temperate Phragmites-dominated marsh: effect of growth stage and plant-mediated
513 transport. Global Change Biol, 5(4): 433-440.
514 Kljun, N., Kastner-Klein, P., Fedorovich, E. and Rotach, M.W., 2004. Evaluation of Lagrangian
515 footprint model using data from wind tunnel convective boundary layer. Agric. Forest
516 Meteorol., 127(3-4): 189-201.
517 Larson, J.H. et al., 2013. Great Lakes rivermouth ecosystems: Scientific synthesis and
518 management implications. Journal of Great Lakes Research, 39(3): 513-524.
519 Le Mer, J. and Roger, P., 2001. Production, oxidation, emission and consumption of methane by
520 soils: A review. European Journal of Soil Biology, 37(1): 25-50.
521 Leppala, M., Oksanen, J. and Tuittila, E.S., 2011. Methane flux dynamics during mire
522 succession. Oecologia, 165(2): 489-499.
523 Matthes, J.H., Sturtevant, C., Verfaillie, J., Knox, S. and Baldocchi, D., 2014. Parsing the
524 variability in CH4 flux at a spatially heterogeneous wetland: Integrating multiple eddy
525 covariance towers with high-resolution flux footprint analysis. J. Geophys. Res.
526 Biogeosci., 119(7): 1322-1339.
527 McCarthy, M.J. et al., 2007. Effects of hydrological flow regime on sediment-water interface and
528 water column nitrogen dynamics in a great lakes coastal wetland (Old Woman Creek,
529 Lake Erie). Journal of Great Lakes Research, 33(1): 219-231.

McLeod, E. et al., 2011. A blueprint for blue carbon: toward an improved understanding of the role of vegetated coastal habitats in sequestering CO2. Frontiers in Ecology and the Environment, 9(10): 552-560.

Michalak, A.M. et al., 2013. Record-setting algal bloom in Lake Erie caused by agricultural and meteorological trends consistent with expected future conditions. PNAS, 110(16): 6448-6452.

Mitsch, W.J. et al., 2013. Wetlands, carbon, and climate change. Landscape Ecology, 28(4): 583-597.

Moffat, A.M. et al., 2007. Comprehensive comparison of gap-filling techniques for eddy covariance net carbon fluxes. Agric. Forest Meteorol., 147(3-4): 209-232.

Morin, T.H. et al., 2014a. Environmental drivers of methane fluxes from an urban temperate wetland park. J. Geophys. Res. Biogeosci., 119(11): 2014JG002750.

Morin, T.H. et al., 2014b. The seasonal and diurnal dynamics of methane flux at a created urban wetland. Ecological Engineering, 72: 74-83.

Morin, T.H. et al., 2017. Combining eddy-covariance and chamber measurements todetermine the methane budget from a small, heterogeneous urbanfloodplain wetland park. Agric. Forest Meteorol., 237: 160-170.

Morrissey, L.A., Zobel, D.B. and Livingston, G.P., 1993. Significance of stomatal control on methane release from Carex-dominated wetlands. Chemosphere, 26(1-4): 339-355.

Nahlik, A.M. and Mitsch, W.J., 2010. Methane Emissions From Created Riverine Wetlands. Wetlands, 30(4): 783-793.

551 Reichstein, M. et al., 2005. On the separation of net ecosystem exchange into assimilation and
552 ecosystem respiration: review and improved algorithm. Global Change Biol, 11(9): 1424-
553 1439.
554 Sachs, T., Giebels, M., Boike, J. and Kutzbach, L., 2010. Environmental controls on CH4
555 emission from polygonal tundra on the microsite scale in the Lena river delta, Siberia.
556 Global Change Biol, 16(11): 3096-3110.
557 Segers, R., 1998. Methane production and methane consumption: a review of processes
558 underlying wetland methane fluxes. Biogeochemistry, 41(1): 23-51.
559 Sha, C. et al., 2011. Methane emissions from freshwater riverine wetlands. Ecological
560 Engineering, 37(1): 16-24.
561 Tokida, T. et al., 2007. Falling atmospheric pressure as a trigger for methane ebullition from
562 peatland. Global Biogeochemical Cycles, 21(2).
563 Tomaszek, J.A., Gardner, W.S. and Johengen, T.H., 1997. Denitrification in sediments of a Lake
564 Erie coastal wetland (Old Woman Creek, Huron, Ohio, USA). Journal of Great Lakes
565 Research, 23(4): 403-415.
566 Updegraff, K., Pastor, J., Bridgham, S.D. and Johnston, C.A., 1995. Environmental and substrate
567 controls over carbon and nitrogen mineralization in northern wetlands. Ecological
568 Applications, 5(1): 151-163.
569 Wang, Z.P., Delaune, R.D., Masscheleyn, P.H. and Patrick, W.H., 1993. Soil redox and ph
570 effects on methane production in a flooded rice soil. Soil Sci. Soc. Am. J., 57(2): 382-
571 385.

572 Webb, E.K., Pearman, G.I. and Leuning, R., 1980. Correction of flux measurements for density
573 effects due to heat and water-vapor transfer. Quarterly Journal of the Royal
574 Meteorological Society, 106(447): 85-100.
575 White, J.R., Shannon, R.D., Weltzin, J.F., Pastor, J. and Bridgham, S.D., 2008. Effects of soil
576 warming and drying on methane cycling in a northern peatland mesocosm study. J.
577 Geophys. Res. Biogeosci., 113.
578 Whyte, R.S., Trexel-Kroll, D., Klarer, D.M., Shields, R. and Francko, D.A., 2008. The Invasion
579 and Spread of Phragmites australis during a Period of Low Water in a Lake Erie Coastal
580 Wetland. Journal of Coastal Research: 111-120.

581